# MODEL BASED BATTERY MANAGEMENT SYSTEM FOR CONDITION BASED MAINTENANCE

Nick Williard, Wei He, and Prof Michael Pecht
Center for Advanced Life Cycle Engineering
Room 1101 Eng. Lab. Bldg 89
University of Maryland
College Park, MD 20742
Telephone: 301-405-5323
Pecht@calce.umd.edu

**Abstract:** A generalized approach for combining state of charge (SOC) and state of health (SOH) techniques together to create a self-adaptive battery monitoring system is discussed. First, previously published techniques and their feasibility for on-line SOC and SOH estimation are reviewed. Then, a method of utilizing SOH predictions to update the SOC estimator in order to minimize drift due to capacity loss and cell degradation is given. This method is demonstrated by combing an equivalent circuit model to estimate SOC with an empirical/data driven model of capacity fade to estimate SOH. The method is validated with data obtained through cycle life testing of a lithium-ion battery. Parameters for the equivalent circuit model are initially extracted from electrochemical impedance spectroscopy data and are updated by least squares fitting and future SOH predictions. Lastly the results of SOC and SOH estimations are translated into terms that can be easily interpreted by an electric vehicle user so that the presented method can be implemented into an onboard fuel gauge and condition based maintenance system.

**Key words:** Battery management system; health management; prognostics; state of charge; state of health

**Introduction:** The rising discipline of prognostics and health management (PHM) is realizing applications in many of today's state of the art technologies to help predict and mitigate failure. This is achieved by combining sensing and interpretation of environmental, operational, and performance-related parameters to assess the health of a product and predict remaining useful life. One of the most promising and ready technologies for application of PHM methods into field operation are lithium-ion battery management systems (BMS). These systems are put into place in order to provide system state information, optimized performance, and improved safety for users of battery operated systems.

A critical BMS function is to provide the user with battery state estimations and predictions. In both industry and academia two major topics of interest are determination of the state of charge (SOC) and state of health (SOH). SOC refers to the amount of remaining charge in a battery which provides the user with important information on system run-time before a battery recharge is required. In an electric vehicle the SOC

information is presented as the fuel gauge; in a cell phone this information is presented as the battery life bar. SOH refers to the amount of degradation that has occurred in a battery compared to the beginning of life. SOH can be used to update the SOC so that changes in battery discharge properties due to degradation are reflected in the remaining charge predictions. By taking the concept of SOH one step further and modeling degradation so that SOH estimations can be projected into the future, we can estimate a battery's remaining useful cycle life performance (RUP) or state of life (SOL). RUP predictions can be implemented as part of a condition based maintenance strategy for planning battery replacements.

Many of the problems associated with state estimations exist due to the inherent uncertainties of battery dynamics. Slight variations in material processing and particle contaminates in raw materials can lead to different degradation trends even under a tight quality control regiment. Battery degradation also varies widely due to the complex relationships between usage profiles and environmental conditions. In order to overcome these challenges, PHM seeks to track and characterize this degradation in real time and autonomously learn the behavior of each individual battery.

Figure **1** proposes a generalized process flow for performing battery state estimations. This process must operate over two different time scales. For SOC, estimations are made over the course of one discharge cycle which may range from minutes to days depending on the current load and the charge capacity of the battery. The SOC can be determined by developing a relationship between SOC and the terminal voltage of the battery. For this, a battery voltage model is required. For SOH, estimations are made over the charge/discharge cycle life of the battery which can last on the order of months or years depending on the application and the cycle life characteristics of the battery. SOH can be determined by evaluating the amount of capacity fade that has occurred in the battery. Determination of capacity fade requires a separate model which can be data driven or developed based on the physical degradation processes that occur within a battery.

The process flow in

Figure **1** shows how predictions from the SOH and SOC models feed into each other to create an accurate and adaptive system. The SOC estimations require a prediction of the battery's maximum capacity at the beginning of discharge. However, in order to directly measure a battery's capacity, it must undergo a discharge. This presents a problem as the capacity of some cycle $n$ is not known until the end of the $n^{th}$ discharge. Therefore, at the beginning of the next cycle we must make an estimation of the cycle $n+1$ capacity. This can be gained by updating the capacity fade model based on the $n^{th}$ discharge data and then extrapolating the capacity fade model one cycle into the future. When more data has been collected during the $n+1$ cycle, the parameters of the voltage model can be adjusted in order to fit the observed data and provide a better estimate of the capacity for that discharge cycle. This updated capacity can then be compared with the original $n+1$ capacity prediction to update the parameters of the capacity fade model. Though constant

estimation, prediction, and refinement of the discharge voltage and capacity fade models real time updates of SOC and SOH can be made.

The following sections review different voltage and capacity fade models that have been proposed in literature. The benefits and drawbacks of implementing these models onboard real life BMSs are discussed. Then, two widely used filtering techniques for updating model parameters are reviewed.

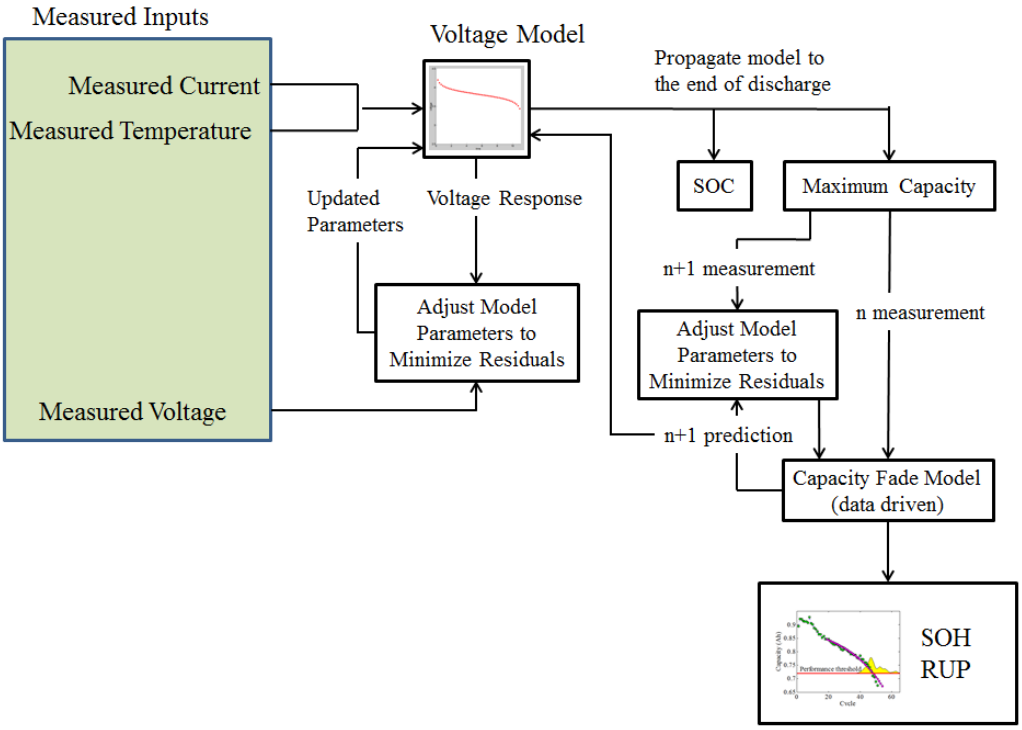


Figure 1: Generalized Process Flow for Battery State Estimation

**Voltage Models:** Several voltage models for lithium ion batteries exist. Fundamental work on this topic was performed by Fuller, Doyle and Newman [1] who used concentrated solution theory to describe ion transport through the electrolyte, and Duhamel's superposition integral on a series of step changes in ion surface concentration to determine ion flux into the electrodes. Because voltage is related to the ion concentration in each electrode, voltage profiles can be determined from this species transport model. While this, and other first principle voltage models [2,3] have proved useful for design optimization and performance prediction, their computational intensity and large number of input variables which are not readily measurable, make them undesirable for in-situ monitoring.

To overcome the difficulties associated with implementing high order physics based simulations into real time applications, several simplified models have been proposed. Subramanian et al. [4] simplified the solid-phase concentration by only considering $Li^+$ surface and the average concentrations to determine SOC. These equations were obtained using polynomial approximation and volume-average integration. Dao et al. [5] approximated the electrolyte phase concentration using the Galerkin method with a

sinusoidal trial function. Once all the phase concentrations where known a constant current density was assumed and the Butler-Volmer equations were used to determine the solid and electrolyte over-potentials. Other simplifications can be realized by modeling the electrodes as a single sphere known as the single particle (SP) model [6,7]. The SP simplification assumes that contributions to cell kinetics due to the solution phase are negligible. The concentration inside the sphere is approximated by a parabolic profile which like in ref [4] is expressed in terms of the average and surface $Li^+$ concentrations.

Further simplifications can be made through the use of an equivalent circuit model. Rather than first principles modeling of battery dynamics, equivalent circuit models (ECM) assume that batteries exhibit resistive and capacitive electrical properties which can be simulated by an RC circuit. While ECMs are much higher level models (and much more simple to solve compared to the ordinary differential equations required for first principles modeling), they can still provide insights into the battery's internal operating mechanisms. A well-developed ECM can include a component for each factor that has an electrical influence within the cell structure. For example, a resistor can be used to account for the resistance between each particle within the electrode structure. This could be put in series with a resistor and capacitor in parallel which describes the properties of the electrode/electrolyte interface where the resistor would model the resistance due to electrode surface films and the capacitor would describe the capacitive properties of ions moving from the electrode surface double layer into the electrode itself.

ECMs are often validated through the use of electrochemical impedance spectroscopy in which the electrical parameters of the ECM are extracted from the Nyquist plot generated by the battery. The resistance due to the electrolyte $R_p$ is determined to be the real part of the impedance where the semi-circle first crosses the x-axis, the real part of the impedance where the semi-circle crosses the x axis for the second time is considered to be the sum of $R_p$ and $R_{ct}$ where $R_{ct}$ is considered to be the charge transfer resistance at the surface of the electrode. The double layer capacitance which is the capacitive element on the electrode surface can be evaluated by:

$$C_{dl} = \frac{1}{\omega R_{ct}} \tag{1}$$

where ω is the frequency at which the top of the semi-circle is evaluated. By evaluating the equivalent circuit, a time and current dependent voltage equation can be determined which fits the electrical response of the battery. Many equivalent circuit models have been proposed and demonstrated on lithium ion cells [8,9,10,11,12,13].

**Capacity Fade Models:** Capacity fade modeling presents similar challenges to voltage modeling. Physics based models are preferred for their ability to capture battery degradation under a wide range of usage and environmental conditions without the need for a significant amount of training data. However, their applications are limited by their requirements for a large number of difficult to measure input parameters. In order to account for model uncertainties, these parameters must be constantly measured and updated in real time which is best performed by only considering the parameters which are most effected by battery degradation. Additional complications in capacity fade

modeling arise due to the fact that battery degradation can be caused by several different internal mechanisms [14]. Modeling all of these internal mechanisms simultaneously further increases model complexity. Therefore physics based capacity fade models generally only consider the effects of a small number of these possible mechanisms.

Ramadass et al [15] developed a first principles capacity fade model by only considering the mechanism of solvent reduction during charging to account for the loss of capacity. Here it was assumed that the charge transfer current density was a summation of the intercalation and side reaction current densities. Then, Butler-Volmer kinetics was used to calculate the rate of solvent reduction and corresponding rate of surface film thickening. The increased internal resistance due to the thickening of these surface films resulted in the reduction of capacity. Schmidt et al [16] used a simplified lumped parameter electrochemical battery model to determine capacity fade. The model was applied to a single representative particle in the cathode and anode. In this work capacity fade was attributed to the reduction of cathode's effective porosity while the reduction of capacity due to anode degradation was neglected. The reduction in porosity with increased usage results in a decreased ability for the cathode to store lithium ions and hence results in capacity fade. This model was developed particularly for online state estimation and used the least squares approach to fit the modeled parameters to the measured data. He et al [17] developed an empirical exponential model for online capacity fade prediction. The model described the maximum battery capacity and was dependent on cycle number. Four model parameters were adjusted to fit observed capacity data using a Bayesian Monte Carlo approach. The model was able to generate a probability density function for the predicted SOL.

**Experimental:** To evaluate the process flow described in

Figure **1**, a commercial single cell lithium ion battery underwent charge/discharge cycling. The cell had a rated capacity of 1.1Ah and was composed of standard materials typically found in batteries for portable electronics. The cathode was composed of $LiCoO_2$ particles adhered to an aluminum current collector with a polymer binder. The anode was composed of graphite particles which were deposited on a copper current collector. The electrodes were separated by a polymer matrix and the whole cell was doused in a solution of $LiPF_6$ dissolved in organic solvents to provide the electrolyte.

Cycle life testing was performed using an Arbin BT2000 battery test system. During charging the constant current constant voltage charging protocol was used. This applied a constant current of 0.55A to the battery until its terminal voltage reached 4.2V, then the charger switched to a constant voltage mode where the terminal voltage of the battery was held at 4.2V until the charging current dropped to below 0.05A. The constant voltage mode is a "top-off" step that allows the terminal voltage to approach the open circuit voltage in the battery. After charging, the battery was discharged at a constant current of 0.55A until the terminal voltage of the battery reached the cut-off voltage threshold of 2.7V. Throughout cycling the current, terminal voltage and time data was sampled every 30 seconds by the battery test system. It should be mentioned that while

the following methods were performed on data collected by the battery test system, in real life applications data would need to be collected though some data acquisition module such as the one described in [18]. An entire PHM system would consist of a data acquisition module, a processer for computing the following algorithms, and a user interface to display the results to the user.

**Case Study:** The voltage of the above mentioned battery was modeled using the equivalent circuit method derived in [12]. A schematic of the equivalent circuit used is shown in Figure 2. From this we get the following time and current dependent equation for the terminal voltage of a battery under constant current discharge.

$$V(t; I\ constant) = \frac{Q(0)}{C}\, e^{-t/(R_2 C)} + V_o - IR_1 - IR_2[1 - e^{-\frac{t}{R_2 C}}] \qquad (2)$$

where $R_1$, $R_2$, and $C$ are the resistive and capacitive components respectively of the chosen equivalent circuit, $I$ is the current, $Q(0)$ is the initial electrical charge stored within the battery (the battery's initial capacity), $t$ is time, and $V_o$ is the open circuit voltage.

The values of $R_1$, $R_2$, and $C$ were extracted from impedance spectroscopy data Figure 3 as described in the *voltage models* section. The values are shown in Table 1. Impedance spectroscopy was performed on the battery at the beginning of life as a characterization step and is not meant to be part of the on board prognostics system as the equipment is too large and burdensome to be feasibly incorporated into a real world battery management system.

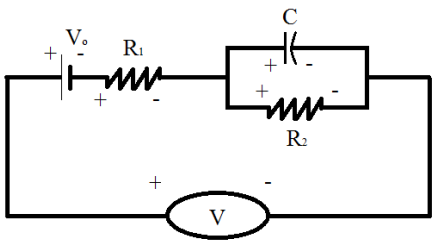


Figure 2: Schematic of Equivalent Circuit

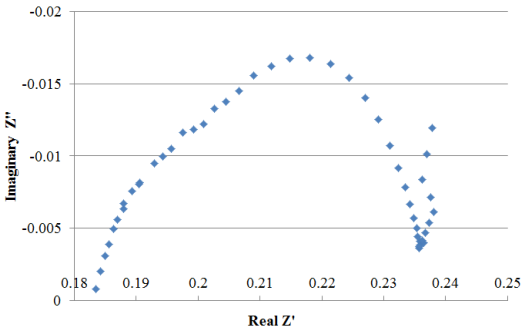


Figure 3: Nyquist Plot

Table 1: extracted ECM values

| Component | Value |
|---|---|
| **$R_1$** | **0.18Ω** |
| **$R_2$** | **0.06 Ω** |
| **C** | **30F** |

To determine the initial capacity of the battery *Q(0)*and the open circuit voltage $V_o$ with respect to time a preliminary charge/discharge cycle was conducted at 0.55A. The initial capacity was calculated by integrating the current with respect to the time during discharge:

$$Q(0) = \int_{t_1}^{t_2} Idt \tag{3}$$

where $t_1$ corresponds to the time when the battery was fully charged and $t_2$ corresponds to the time when the battery was fully discharged. The open circuit voltage was calculated by averaging the terminal voltages measured during charging and discharging as shown in Figure 4. This allows for the minimization of terminal voltage effects associated with hysteresis and ohmic resistance. For computational purposes, the values of open circuit voltage and time were saved in a look up table. When using $V_o$ in the voltage model the appropriate values were determined through linear interpolation of the look up table to find the correct voltage value for each time during discharge.

Figure 5 shows the results of the voltage model compared with voltage data collected during the first and 700$^{th}$ cycle. As expected, the model fits best with discharge profiles at the beginning of life before aging effects, such as the rise of internal resistance, alter the discharge curve. In order to account for the effects of aging, capacity fade must be taken into account.

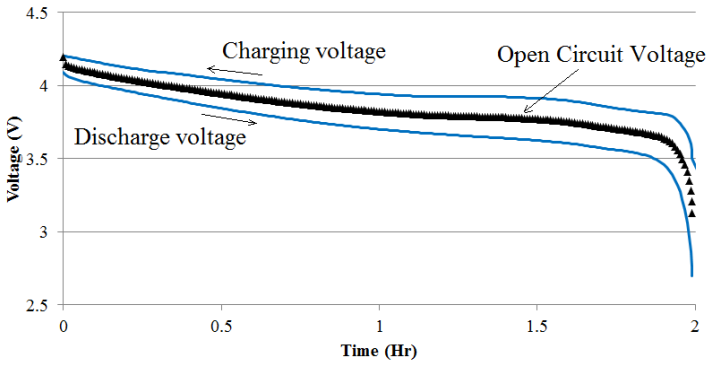


Figure 4: Calculation of OCV

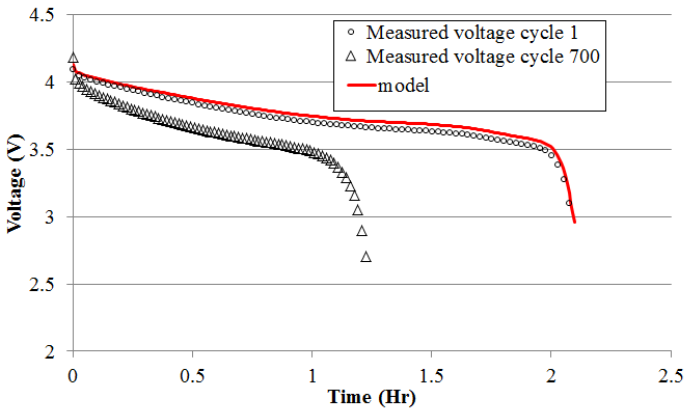


Figure 5: Initial Equivalent circuit model compared to the measured discharge voltage at cycle 1 and 700

For updating the voltage model we continuously adjusted $R_1$, $Q(0)$ and the $V_o$ look up table using the prediction of n+1$^{th}$ cycle capacity. In the current work capacity fade predictions were made using the model proposed by He et al. [17]:

$$Q = a \cdot \exp(b \cdot n) + c \cdot \exp(d \cdot n) \tag{4}$$

where $Q$ is the capacity, $n$ is the cycle number, and $a$,$b$,$c$, and $d$ are model parameters that should be updated at the end of each discharge so that the model best reflects the measured capacity. To update the model parameters as indicated by the "adjust model parameters to minimize residuals" loops in

Figure **1**, we will use the Unscented Kalman Filter (UKF) [19, 20].

UKF is a specific application of the unscented transform. In unscented transform a Gaussian random variable is used to approximate a state distribution. To do this, a small set of sample points known as sigma points are chosen which can capture the mean and covariance of the Gaussian random variable. These sigma points can then be propagated though a nonlinear system in order to capture the true parameter values in the presents of noisy input data. In the current work we propagate the parameter vector x as a random variable through the nonlinear capacity function, Q = g(x) assuming that x has mean $\bar{\mathbf{x}}$ and covariance $\mathbf{P}_x$.

The results of applying UKF at the end of every discharge cycle to predict the n+1 capacity are shown in Figure 6. UKF was able to provide sufficient next step predictions with a root-mean-square error of 1.04% as the battery capacity degraded in a non-linear fashion.

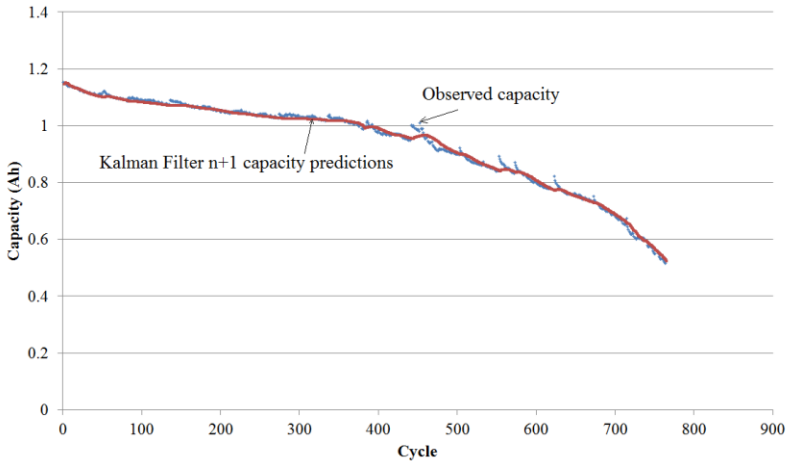


Figure 6: results of UKF on capacity fade data

To update the voltage model, the n+1$^{th}$ cycle capacity calculated at the end of the n$^{th}$ cycle is substituted for *Q(0)* in the voltage equation. To update the OCV look up table, the values of OCV were assumed to remain constant throughout cycle life, however the time corresponding to each voltage value was updated so that the time for the end of discharge corresponded with the appropriate discharge cut-off voltage. Because discharge was performed at a constant current, the time for end of discharge was calculated by dividing the capacity by the discharge current. Then, for *k* number of values in the OCV look up table, the time values were determined as:

$$T = [1 \cdot \frac{Q}{i \cdot k}, 2 \cdot \frac{Q}{i \cdot k}, 3 \cdot \frac{Q}{i \cdot k}, \dots, k \cdot \frac{Q}{i \cdot k}] \tag{5}$$

where *Q/i* is the time to the end of discharge. To determine the value of $R_1$ at the end of each discharge, non-linear least squares regression was used to find the value of $R_1$ such that the residuals between the voltage equation and the measured voltage values were minimized. Previous work [21] has suggested a linear relationship exists between internal resistance and capacity so as cycling progressed a linear relationship between resistance and capacity was established using linear least squares regression. This relationship was found to be:

$$R_1 = -0.5349 \cdot Q + 0.7684 \tag{6}$$

which was used to update the values of $R_1$ as battery degradation progressed. Using this relationship to update $R_1$ while using EKF to update *Q(0)* and the $V_o$ look up table, we were able to provide a good fit between the voltage model and the measured voltage data throughout the battery's cycle life. Figure 7 shows the model fit to the voltage data for cycle 1, cycle 400, and cycle 700. It can be seen that while the model slightly over predicts the voltage in the beginning of life, it is still able to adapt as the battery undergoes aging.

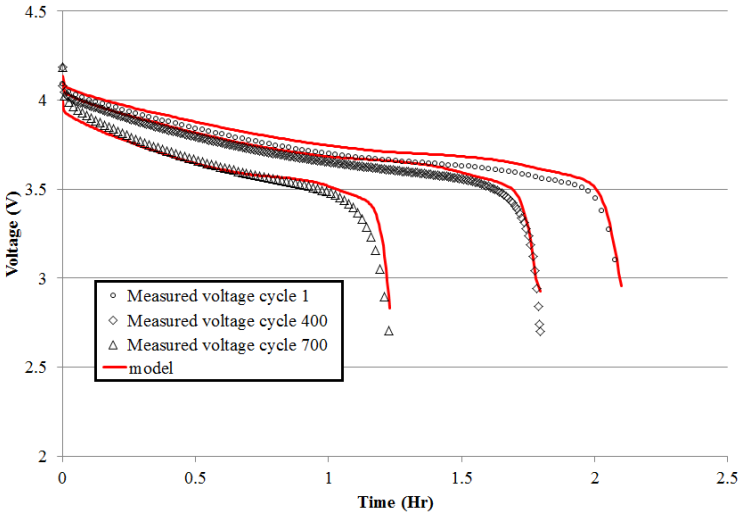


Figure 7: Modeled voltage curve with measured voltage data at 3 different discharges throughout cycle life

**Interpreting State Estimation:** Voltage and capacity fade modeling alone provide little value to users outside the technical community. Because these methods are meant to translate information to users of electric vehicles and portable electronics, they must be translated into terms that are familiar to the general population. The first step in interpreting voltage and capacity fade, is to translate these terms into SOC and SOH respectively.

With an updated voltage profile for a given discharge cycle, we can then describe the system SOC by creating a look up table which gives a 0 to 1 mapping of the predicted discharge voltage where 1denotes the SOC of the battery when the voltage is at its maximum charge voltage (4.2V in this case) and a SOC of 0 corresponds to the minimum discharge voltage (2.7). Figure 8 shows the battery discharge voltage with its corresponding SOC versus discharge time. The SOC mapping is helpful because it provides a linear path with respect to usage between a "full" battery and an "empty" battery. In vehicle applications, because the user has become accustom to evaluating the remaining driving time by associating it with a fuel gauge, the SOC of a battery should be correlated with the rotation of a fuel gauge needle so that at an SOC of 0 the needle is aligned with the empty mark and at an SOC of 1 the needle is aligned with the full mark.

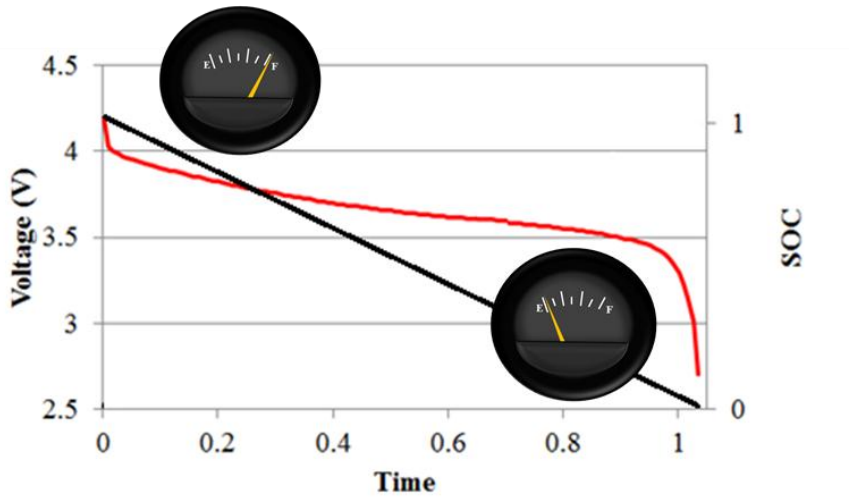


Figure 8: Plot of the discharge voltage (red) and the corresponding SOC mapping (black)

In the case of the SOH problem, we can determine the SOH by comparing the capacity at the beginning of life to the capacity at some cycle *k*:

$$SOH = \frac{Q_{max}(k)}{Q_{max}(1)} \tag{7}$$

where $Q_{max}$ represents the maximum discharge capacity at a particular cycle. In the case of SOH there is not an equivalent analogy which is currently in place in gasoline powered vehicles. Today's vehicles use indicators such as "check engine" lights to warn users of impending hard failures which could result the breakdown of the vehicle. In future electric vehicles, while hard failures are still a concern (as was realized with the recent battery fires in the Chevy Volts), long term stable operation of will likely lead to significant capacity fade before a hard failure. Capacity loss results in a shorter discharge time, which in an electric vehicle has the effect of a shrinking gas tank as depicted in Figure 9. In order to convey this information to the user a new indicator may need to be conceived.

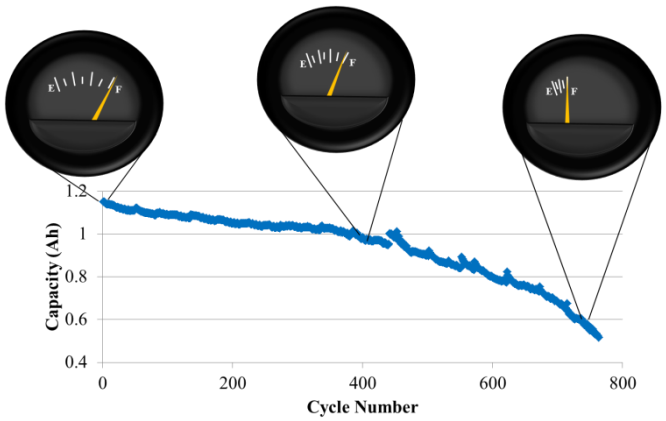


Figure 9: Reduction of available charge as capacity decreases with usage

The SOH indicator may also provide useful to technicians inspecting failed batteries. Because the degradation trend of batteries varies from cell to cell, there is the potential that a limited number of cells in an electric vehicle battery pack could be responsible for a majority of lost charge. If SOH monitoring could be applied to each cell individually, this would give the technician an indication of which cells needed to be replaced. This type of maintenance could save a substantial amount of money if battery packs were designed so that individual cell replacement could be easily performed.

**Conclusion:** This paper outlined a general framework for estimating both SOC and SOH within the same process flow. This processes flow is generalized to the point where any of the available voltage and capacity models can be combined together in order to produce a self-updating state estimator. In the current paper a standard equivalent circuit SOC approach was combined with an empirical/data driven SOH approach. Additionally, the value and purpose of battery state estimation as it pertains to the operation and maintenance of electric vehicles by a layman user was discussed.

**References**


1. Thomas F. Fuller, Marc Doyle, and John Newman, J. Electrochem. Soc., 141 (1994), 1-10.
2. Marc Doyle, Thomas F. Fuller, and John Newman, J. Electrochem. Soc., 140 (1993), 1526-1533.
3. Thomas F. Fuller, Marc Doyle, and John Newman, J. Electrochem. Soc., 141 (1994), 982-990.
4. V. Subramanian et al./ Journal of The Electrochemical Society, **152** 10 (2005) A2002-A2008
5. T.-S.Dao et al. / Journal of Power Sources *198 (2012) 329– 337*
6. B.S. Haran et al. / Journal of Power Sources 75 (1998) 56–63
7. S. Santhanagopalan et al. / Journal of Power Sources 156 (2006) 620–628
8. B.Y. Liaw et al. / Solid State Ionics 175 (2004) 835-839
9. Y.-M. Choi et al. / Solid State Ionics 99 (1997) 173-183
10. M. Mirzaeian et al. / Journal of Power Sources 195 (2010) 6817-6824
11. M. Xu et al. / Electrochimica Acta 50 (2005) 5473-5478
12. M. Verbrugge. Journal of the Electrochemical Society 149 (2002) A45-A53
13. S.K. Rahimian et al. / Journal of Power Sources *196 (2011) 8450– 8462*
14. N. Williard et al. / J Mater Sci: Mater Electron (2011) 22:1616–1630
15. P. Ramadass et al/ *Journal of The Electrochemical Society*, **151** (2004) A196-A203
16. A.P. Schmidt et al/ Journal of Power Sources 195 (2010) 7634-7638
17. W. He et al/ Journal of Power Sources 196 (2011) 10314-10321
18. Z. Taha et al. / Mechatronics 21 (2011) 132–144
19. F Zhang et al/ Battery State Estimation Using Unscented Kalman Filter, IEEE International Conference on Robotics and Automation May 12-17, 2009
20. E.A. Wan and R. Van Der Merwe. The Unscented Kalman Filter for Nonlinear Estimation," in The IEEE Adaptive Systems for Signal Processing,

Communications, and Control Symposium 2000, Lake Louise, Alberta, Canada, Oct. 2000, pp. 153 - 158.
21. Goebel et al./ Prognostics in Battery Health Management. IEEE Instrumentation & Measurement Magazine. August 2008